PROCEEDINGS OF SCIENCE

NNLO predictions for dijet production in diffractive DIS

Radek Žlebčík*
DESY
E-mail: radek.zlebcik@desy.de

Daniel Britzger
Physikalisches Institut, Universiät Heidelberg
E-mail: britzger@physi.uni-heidelberg.de

James Currie
Institute for Particle Physics Phenomenology, Durham University
E-mail: james.currie@durham.ac.uk

Thomas Gehrmann
Department of Physics, University of Zürich
E-mail: thomas.gehrmann@uzh.ch

Alexander Huss
Institute for Theoretical Physics, ETH, Zürich
E-mail: ahuss@phys.ethz.ch

Jan Niehues
Institute for Particle Physics Phenomenology, Durham University
E-mail: jan.m.niehues@durham.ac.uk

The cross sections fo the dijet production in diffractive deep-inelastic scattering are calculated for the first time in next-to-next-to-leading accuracy. The next-to-next-to-leading order corrections are found to be positive and sizable. The cross sections are compared to a considerable number of HERA measurements performed by H1 and ZEUS collaborations. We observe an overall good agreement of the next-to-leading order calculation with data, whereas the next-to-next-to-leading calculations tend to overestimate the data, probably due to poorly constrained gluon component of the diffractive parton distribution functions.

XXVI International Workshop on Deep-Inelastic Scattering and Related Subjects (DIS2018)
16-20 April 2018
Kobe, Japan

*Speaker.

PoS(DIS2018)059

1. Introduction

Diffractive processes, $ep \to eXY$, where the systems X and Y are separated in rapidity, have been studied extensively at the electron-proton collider HERA. The forward system Y usually consists of the leading proton but can also contain its low mass dissociation. Between the systems X and Y is a depleted region without any hadronic activity (large rapidity gap) which is a consequence of the vacuum quantum numbers of the diffractive exchange, often referred to as a pomeron ($I\!P$). Experimentally, diffractive events can be selected either by requiring a rapidity region without any hadronic activity (large rapidity gap method) or by direct detection of the leading proton. In the second case, the system Y is free of any diffractive dissociation.

In analogy to the non-diffractive case, also in diffraction parton distribution functions can be defined. According to the factorisation theorem [1] the diffractive cross section is then expressed as a convolution of these diffractive densities (DPDF) and partonic cross sections of the hard subprocess which are calculable within perturbative QCD. The DPDFs have properties similar to the classical PDFs, especially they obey the DGLAP evolution equation, but have an additional constraint on the presence of the leading proton in the final state.

Within the diffractive factorisation frame the DPDFs are extracted from the reduced cross sections of inclusive diffractive DIS [2] which is the process with the highest statistics. Consequently these DPDFs are used to predict cross sections of other, more exclusive, processes in DIS. At HERA, due to relatively small masses of system X, only the dijet cross sections and D^* cross sections were measured. As the gluonic component of DPDFs is weakly constrained from the inclusive measurement both H1 and ZEUS collaborations performed also a combined fit of inclusive and dijet data [3, 4] where the dijet cross section allows for a better constraint of the gluon DPDF component.

Up to now, the diffractive data were compared only to the leading-order (LO) and next-to-leading order (NLO) QCD predictions based on the collinear factorisation theorem. We present the next-to-next-to-leading order (NNLO) predictions for the diffractive processes for the first time. These predictions were calculated for dijet production in diffractive DIS and were confronted with 6 measurements published by the H1 or ZEUS collaborations. More details are given in Ref. [5].

2. Variable definition

The cross sections are studied differentially in several kinematic variables which are also used to constrain the phase space of the measurement. The standard DIS observables are the photon virtuality $Q^2 = -q^2$ ($q = k - k'$) and the inelasticity y defined as $y = \frac{pq}{pk}$, where the incoming proton four-momentum is labeled as p and k (k') denotes the incoming (scattered) electron four-momentum. The jets were always identified using the k_T-algorithm in the $\gamma^* p$ frame with the parameter $R = 1$ and the transverse momentum and pseudo-rapidity, either in $\gamma^* p$ or in the laboratory frame are measured. In almost all analyses, in addition, the diffractive variables $x_{I\!P}$ and $z_{I\!P}$ were measured. The variable $x_{I\!P}$ is a relative energy loss of the beam proton caused by the diffractive scattering and $z_{I\!P}$ can be interpreted as the momentum fraction of the parton entering the hard subprocess with respect to the diffractive exchange (pomeron).

PoS(DIS2018)059

3. NNLO calculations

The theoretical NNLO QCD predictions for dijet production in diffractive ep are calculated using the NNLOJET program [6] based on the antenna subtraction method. In this way the infrared divergences from real-real, real-virtual and virtual-virtual contribution are correctly handled using local subtraction terms. The hard-scattering NNLO matrix elements were previously successfully used for predictions of jet cross sections in non-diffractive DIS [7].

Both, the H1 and ZEUS collaborations published their data corrected for the effects of QED radiation. However, to compare the data with our fixed-order predictions, the so-called non-perturbative corrections must be applied to correct for effects of hadronisation. For the present analysis, the non-perturbative correction factors as provided by the experiments are used.

As the NNLO calculations are very computation-time consuming (more than 100,000 CPU hours) we are using the fastNLO framework [8] to perform the final convolution of the hard sub-process cross section with the DPDFs and α_s. The advantage of this approach is that the costly calculation of the table containing hard-process cross sections for values of x, Q^2 and p_T is performed only once. Consequently the hard process can be easily convoluted with various PDFs, scale choices or α_s values.

4. Results

We calculated the cross sections at NNLO accuracy for 6 phase space regions related to 6 data analyses of H1 and ZEUS collaborations. In the plots they are are labeled with the following name tags: H1 FPS (HERA II) [9], H1 VFPS (HERA II) [10], H1 LRG (HERA II) [11], H1 LRG (HERA I) [3], H1 LRG (300 GeV) [12], ZEUS LRG (HERA I) [13]. Five of them are performed with a proton beam energy of 920 GeV, one of them has a smaller energy of 820 GeV. The electron beam energy is always 27.6 GeV. In two of these measurements the leading proton is directly detected by the Forward Proton Spectrometer (FPS) or Very Forward Proton Spectrometer (VFPS), whereas in other cases the diffractive events are selected using the large rapidity gap method. The exact phase space definition of each of these measurements can be found in the corresponding publications.

In general, we observe the that the NNLO corrections to the original NLO predictions are positive and sizable.

Firstly, we focus on the total cross sections. The left plot of Fig. 1 shows that the NNLO QCD predictions are about 30% higher than the NLO one and they mostly overshoot that data (with the exception of ZEUS measurement), while the NLO QCD predictions are always compatible with the data.

The scale uncertainties, obtained by simultaneous variation of the renormalisation and factorisation scale by a factor of 0.5 and 2 are a bit smaller for NNLO predictions.

On the right plot of Fig. 1 we study the dependence of the theoretical cross section on the diffractive parton densities, using H1 2006 Fit A, H1 2006 Fit B [2], H1 2007 Fit Jets [3], ZEUS SJ [4] and MRW [14] DPDFs. Al these densities were extracted at NLO, no NNLO DPDFs exist so far. It can be seen that the DPDFs obtained by the simultaneous fitting of the inclusive and dijet data give in general smaller predictions than the inclusive-only fits. However, the differences between DPDFs fits are mostly covered by the uncertainties of the H1 2006 DPDF Fit B. The DPDF fits

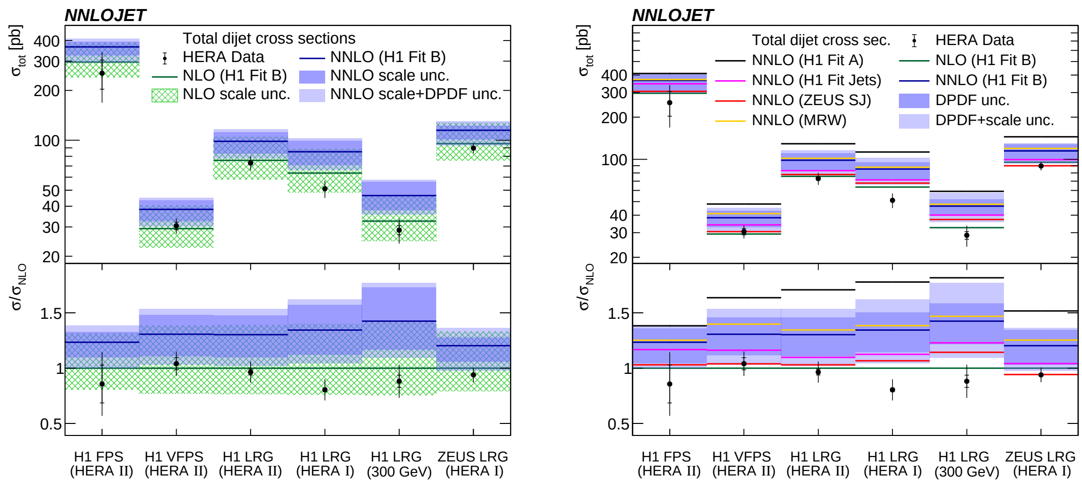

Figure 1: Comparison of the total cross sections of all analysed measurements with theoretical QCD predictions at NLO and NNLO accuracy. The inner data error bars represent statistical uncertainties and other error bars are statistical and systematic errors added in quadrature. On the left, the theoretical predictions using H1 2006 DPDF Fit B are shown with the scale uncertainties (NLO and NNLO) and with scale and DPDF uncertainties added in quadrature (NNLO). In the right plot the NNLO predictions using several DPDF fits are compared. For H1 2006 Fit B NNLO QCD predictions the DPDF and scale uncertainties are depicted.

of only inclusive data [2, 14] have a weakly constrained gluon contribution which is, in particular, visible in case of H1 2006 Fit A which overestimates the jet measurements.

The knowledge of the gluon component of the DPDFs is crucial, as it is demonstrated on the left plot of Fig. 2, which shows that at NNLO a fraction of 85% of the cross section for [11] originates from gluons. In the right plot of Fig. 2, we studied the dependence of the H1 LRG total

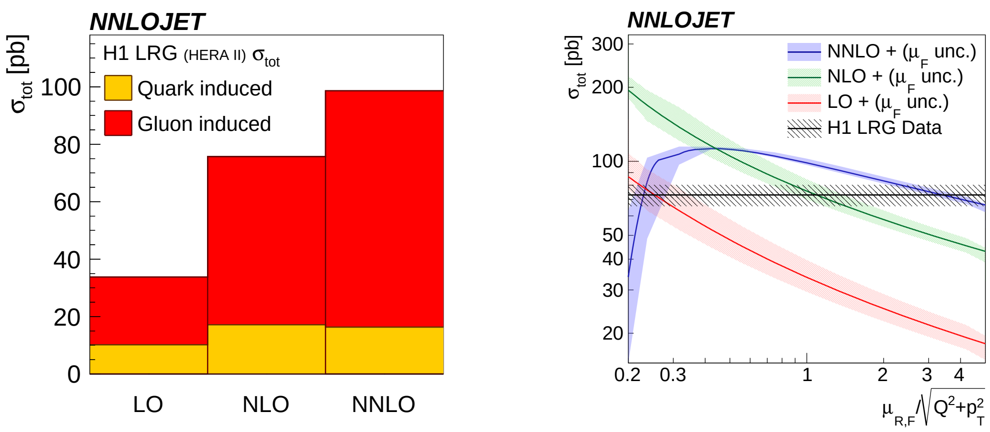

Figure 2: Left: Comparison of the cross section stemming from gluon and quark PDFs, respectively, for the H1 HERA II LRG analysis [11]. Right: The dependence of the total theoretical cross sections at LO, NLO and NNLO on the QCD scale. The uncertainties from factorisation scale variation by the factor of 2 are depicted by the color band. As a reference also the measured data cross section with its uncertainties is plotted.

cross section on the renormalisation and factorisation scales μ_R and μ_F. The nominal value of the scales is $\mu_{R,F} = \sqrt{Q^2 + p_T^2}$, where p_T is the average transverse momentum of the leading and sub-leading jet. In the plot, the renormalisation and factorisation scales are varied simultaneously by a factor from 0.1 to 10 with respect to the nominal value. The effect of having non-equal μ_R and μ_F is studied by varying μ_F between $\mu_F = 0.5\mu_R$ and $\mu_F = 2\mu_R$ and is depicted as the color band. It can be seen that the NNLO cross section is less scale dependent compared to the LO or NLO one. However the prediction overestimates the H1 HERA II LRG data for a wide range of the scale choices. The large scale dependence even at NLO is characteristic for gluon-dominated processes and similar behaviour is observed e.g. for the Higgs boson cross-section.

In total we analysed 40 single- and double-differential distributions, here in Fig. 3 only the y (W) variable is shown as an example. These variables are shown together, as in the studied

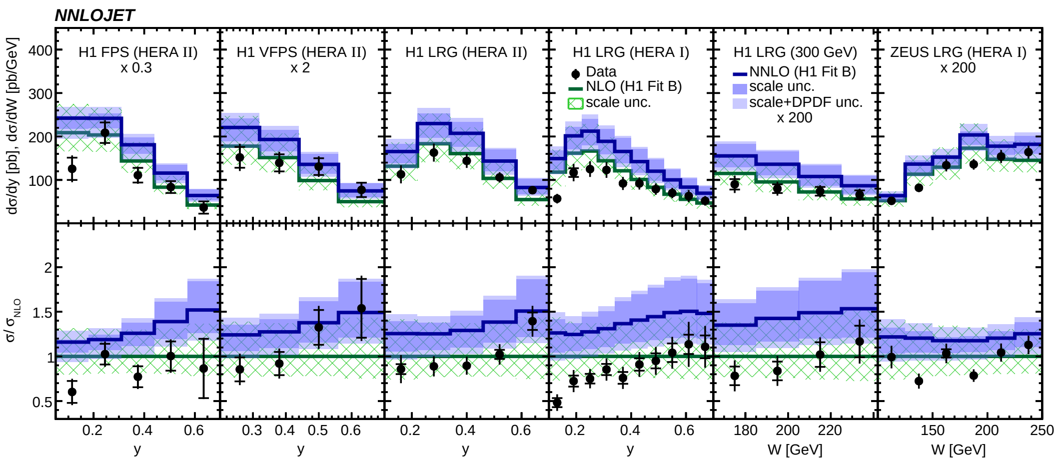

Figure 3: The differential cross section for inelasticity y or $W \simeq \sqrt{ys}$. The pQCD predictions at NLO and NNLO are compared to the data. The scale and the DPDF uncertainties are depicted by the colored bands. To improve readability, some cross sections are multiplied a constant. In addition, the ratio to the NLO pQCD predictions is plotted.

kinematic region W[1] is directly related to y via $W \simeq \sqrt{ys}$, where $\sqrt{s}$ is the centre-of-mass energy. It can be seen that the pQCD predictions based on H1 2006 DPDF Fit B in general overshoot the data. However, the shape of the distributions is better described by the NNLO predictions. To quantify this effect, a χ^2 was calculated for all studied single-differential distributions. The χ^2 is defined in such a way that it does not depend on the theory normalisation and the normalisation is chosen in such a way to get minimal χ^2. The resulting values of the χ^2/ndf are shown in Fig. 4, where the H1 2006 DPDF Fit B was used, but a similar trend was observed also for other DPDFs and/or alternative scale choices as $\mu = p_T$ or $\mu = Q$.

5. Conclusions

We present the first NNLO QCD calculation in diffraction. These predictions were calculated for the dijet production in diffractive DIS and were confronted to 6 measurements published by the

[1] The invariant mass of the $\gamma^* p$ system.

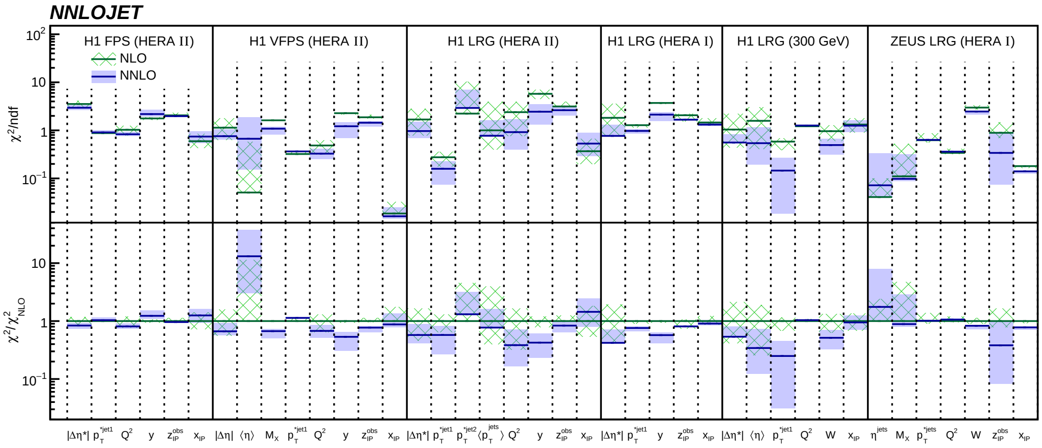

Figure 4: The comparison of the χ^2/ndf, related to the shape agreement between data and NLO or NNLO theoretical predictions based on H1 2006 DPDF Fit B. The color bands represent the scale uncertainty of the pQCD predictions.

H1 or ZEUS collaborations. We observe that the NNLO cross sections are about $\sim 30\%$ higher than NLO calculations. For most of the studied distributions they overshoot the data, but we see that the cross section based on DPDFs from the combined fit of the inclusive and jet data are smaller and agree better than predictions based on inclusive-data-only DPDFs.

The shapes of the differential distributions are better described by NNLO predictions which was quantitatively verified by the χ^2-test. The shape improvement at NNLO was observed for all studied DPDFs and for several choices of the QCD scale.

As no NNLO DPDFs exist, the NLO DPDFs were used to calculate the NNLO predictions. We believe that the normalisation difference data and NNLO predictions could be explained by this inconsistency. To be able to perform calculations in a fully consistent way, the new combined NNLO fit of both, the inclusive and dijet data would be needed. This can verify whether the collinear QCD factorisation theorem holds also for the calculations in the next-to-next-to-leading order accuracy.

References

[1] J. C. Collins, *Proof of factorization for diffractive hard scattering*, *Phys. Rev.* **D57** (1998) 3051 [hep-ph/9709499].

[2] H1 collaboration, A. Aktas et al., *Measurement and QCD analysis of the diffractive deep-inelastic scattering cross-section at HERA*, *Eur. Phys. J.* **C48** (2006) 715 [hep-ex/0606004].

[3] H1 collaboration, A. Aktas et al., *Dijet Cross Sections and Parton Densities in Diffractive DIS at HERA*, *JHEP* **10** (2007) 042 [0708.3217].

[4] ZEUS collaboration, S. Chekanov et al., *A QCD analysis of ZEUS diffractive data*, *Nucl. Phys.* **B831** (2010) 1 [0911.4119].

[5] D. Britzger, J. Currie, T. Gehrmann, A. Huss, J. Niehues and R. Žlebčík, *Dijet production in diffractive deep-inelastic scattering in next-to-next-to-leading order QCD*, *Eur. Phys. J.* **C78** (2018) 538 [1804.05663].

[6] J. Currie, T. Gehrmann and J. Niehues, *Precise QCD predictions for the production of dijet final states in deep inelastic scattering*, *Phys. Rev. Lett.* **117** (2016) 042001 [1606.03991].

[7] H1 collaboration, V. Andreev et al., *Measurement of Jet Production Cross Sections in Deep-inelastic ep Scattering at HERA*, *Eur. Phys. J.* **C77** (2017) 215 [1611.03421].

[8] FASTNLO collaboration, D. Britzger, K. Rabbertz, F. Stober and M. Wobisch, *New features in version 2 of the fastNLO project*, in *Proceedings, 20th International Workshop on Deep-Inelastic Scattering and Related Subjects (DIS 2012): Bonn, Germany, March 26-30, 2012*, p. 217, 2012, 1208.3641, DOI.

[9] H1 collaboration, F. D. Aaron et al., *Measurement of Dijet Production in Diffractive Deep-Inelastic Scattering with a Leading Proton at HERA*, *Eur. Phys. J.* **C72** (2012) 1970 [1111.0584].

[10] H1 collaboration, V. Andreev et al., *Diffractive Dijet Production with a Leading Proton in ep Collisions at HERA*, *JHEP* **05** (2015) 056 [1502.01683].

[11] H1 collaboration, V. Andreev et al., *Measurement of Dijet Production in Diffractive Deep-Inelastic ep Scattering at HERA*, *JHEP* **03** (2015) 092 [1412.0928].

[12] H1 collaboration, A. Aktas et al., *Tests of QCD factorisation in the diffractive production of dijets in deep-inelastic scattering and photoproduction at HERA*, *Eur. Phys. J.* **C51** (2007) 549 [hep-ex/0703022].

[13] ZEUS collaboration, S. Chekanov et al., *Dijet production in diffractive deep inelastic scattering at HERA*, *Eur. Phys. J.* **C52** (2007) 813 [0708.1415].

[14] A. D. Martin, M. G. Ryskin and G. Watt, *Diffractive parton distributions from H1 data*, *Phys. Lett.* **B644** (2007) 131 [hep-ph/0609273].